On the copper oxide neutral cluster distribution in the gas phase: Detection through 355 nm and 193 nm multiphoton and 118 nm single photon ionization

Y. Matsuda, D. N. Shin, and E. R. Bernstein

On the copper oxide neutral cluster distribution in the gas phase: Detection through 355 nm and 193 nm multiphoton and 118 nm single photon ionization

Y. Matsuda, D. N. Shin, and E. R. Bernstein[a]

Department of Chemistry, Colorado State University, Fort Collins, Colorado 80523-1872

The distribution of neutral copper oxide clusters in the gas phase created by laser ablation is detected and characterized through time-of-flight mass spectroscopy (TOFMS). The neutral copper oxide clusters are ionized by two different approaches: Multiphoton absorption of 355 and 193 nm radiation; and single photon absorption of 118 nm radiation. Based on the observed cluster patterns as a function of experimental conditions (e.g., copper oxide or metal sample, ablation laser power, expansion gas, etc.) and on the width of the TOFMS features, one can uncover the true neutral cluster distribution of Cu_mO_n species following laser ablation of the sample. Ablation of a metal sample generates only small neutral Cu_mO_n clusters for $m \lesssim 4$ and $n \sim 1, 2$. Ablation of copper oxide samples generates neutral clusters of the form Cu_mO_m ($m \le 4$) and Cu_mO_{m-1} ($m > 4$). These clusters are directly detected without fragmentation using single photon, photoionization with 118 nm laser radiation. Using 355 and 193 nm multiphoton ionization, the observed cluster ions are mostly of the form $Cu_{2m}O_m^+$ for $4 \le m \le 10$ (193 nm ionization) and $Cu_mO_{1,2}$ (355 nm ionization) for copper oxide samples. Neutral cluster fragmentation due to multiphoton processes seems mainly to be of the form $Cu_mO_{m,m-1} \rightarrow Cu_mO_{m/2,m/2+1}$. Neutral cluster growth mechanisms are discussed based on the cluster yield from different samples (e.g., Cu metal, CuO powder, and Cu_2O powder). © *2004 American Institute of Physics.* [DOI: 10.1063/1.1643894]

I. INTRODUCTION

Metal oxide clusters present a wealth of properties and opportunities for the detailed study of a number of central chemical issues. They have varied properties as a function of cluster size, and one can thus follow their evolution from diatomic molecules to extended systems both experimentally[1–11] and theoretically.[12–15] Their chemical properties are also a function of cluster size, and one can elucidate both reactivity and catalytic behavior for each cluster on an individual basis.[14,16–19] A significant advantage of cluster studies over surface or condensed phase studies is that clusters can be isolated in the gas phase and are thus amenable to individual access both experimentally and theoretically. Such questions as "What are the active sites or species in a heterogeneous catalytic reaction?", "What is the reactivity of the Cu_mO_n cluster?", and "What is the most stable structure for the Cu_mO_n neutral cluster?" can then be addressed in great detail.

In this work, we focus attention on neutral clusters and thus are concerned with careful ionization of the neutral species in order not to cause cluster fragmentation in the ionization process, and thereby loss of information on the neutral clusters present in the gas phase. Ionic clusters, on the other hand, are typically studied by mass selection of individual ion sizes.[16] The study of ionic clusters is thus typically not concerned with cluster fragmentation of a parent species.

Copper oxide and copper-supported metal oxides play an important role in catalytic reactions, including methanol synthesis (H_2/CO),[20] propylene oxidation,[21] and the reduction of NO to N_2,[22] but the detailed microscopic properties of the catalyst in such reactions are unknown. A main path to elucidating the electronic structure and details of catalytically active materials is through cluster studies.

Copper oxide cluster ions have been studied in recent years. Gord *et al.*[3] have investigated collision-induced dissociation of positive and negative Cu_mO_n ions produced by laser desorption/ionization of copper oxide pellets, leading to a determination of $Cu_mO_n^+$ stability. Ma *et al.*[4] have discussed copper oxide cluster cation production by laser ablation processes.

Small neutral clusters have been investigated by anion photoelectron spectroscopy. Wang and co-workers[6] have studied the structure of Cu_2O_x ($x = 1-4$)[5] and CuO_x ($x = 0-6$).[6] Infrared spectra of CuO and CuO_2 have been reported in solid argon matrices by Andrews and co-workers.[23]

The goal of our work is to determine the catalytic behavior of neutral copper oxide cluster toward NO and CO mixtures. As a baseline for these reactivity studies, we need to elucidate the Cu_mO_n neutral cluster distribution generated in our apparatus by laser ablation of a solid sample and subsequent (supersonic) expansion into a vacuum system with high-pressure helium gas. Ionization of the generated neutral clusters is required to determine the neutral cluster distribution and thus, one must investigate the influence of the ionization laser on the observed cluster ion distribution. Ideally, the most gentle ionization is by single photons with energy near the cluster ionization energy threshold. We have em-

a)Electronic mail: erb@lamar.colostate.edu

ployed three laser wavelengths for this process: 355 nm, 193 nm, and 118 nm radiation. Only 118 nm laser light has the requisite energy for gentle single photon photoionization of all the clusters; multiphoton ionization can deposit enough energy into a neutral cluster to cause fragmentation of the parent species following the ionization process.

In this report, we present studies of copper oxide neutral clusters to determine their distribution following laser ablation of metal and metal oxide samples and subsequent supersonic expansion into a vacuum system. The observed cluster distributions are a function of sample preparation, ionization laser timing, power and wavelength, ablation conditions, and other experimental parameters. This study, and the presentation, relies heavily on the recent work from our laboratory on iron oxide neutral clusters.[10,11] Neutral copper oxide clusters are best generated from copper oxide powder samples and are of the form Cu_mO_m for $m \leq 4$ and Cu_mO_{m-1} for the $m > 4$ for the most abundant species. In the presence of multiphoton ionization/fragmentation, these clusters generate ions of the approximate form $Cu_{2m}O_m^+$ $4 \leq m \leq 20$ (193 nm ionization) and Cu_m and $Cu_mO_{1,2}$, $m \leq 10$ (355 nm ionization).

II. EXPERIMENTAL PROCEDURES

The techniques and procedures used here are similar to those reported for our studies of other metal oxide clusters, especially iron oxide.[1,2,10,11] The pulsed supersonic jet of copper oxide is produced by an expansion of laser ablated ($\lambda = 532$ nm, energy/pulse ~ 1 mJ, 10 Hz) copper metal or copper oxide powder with 100% He or 10% O_2/90% He carrier gas at 100 psig, through an orifice of 1 mm diameter into a vacuum chamber (1×10^{-7} Torr with no expansion). Copper foil (99.98%, 0.1 mm) and copper(II) oxide powder (CuO, 99+%) are purchased from Aldrich and copper(I) oxide (Cu_2O, 97%) is purchased from Fisher Scientific (produced by Acros Organics). The copper foil is wrapped around an aluminum drum, and the copper oxide powder is spread and pressed onto a grooved aluminum drum. Copper oxide powder is brittle under these conditions, and it does not adhere well to the drum during an experiment. Thus, a mixture of copper oxide powder with D-glucose (anhydrous) in water (sugar water) and a mixture of copper oxide with glue are also employed as samples that will adhere well to the drum. The sugar is purchased from Mallinckrodt and distilled water is used for the mixture. The glue is made by Elmer's Products, Inc., and is mostly propylene glycol.

Laser radiation is generated by an ArF laser at 193 nm and a Nd/YAG laser for 355 nm and 118 nm. The 355 nm is the tripled Nd/YAG fundamental in a KDP crystal, and this output is used to generate the 118 nm laser ionization beam by tripling in a Xe/Ar gas mixture ($\sim 1:10$) in a static cell at ~ 200 Torr.[11]

Mass spectral features are fit with a Gaussian distribution function in order to determine a linewidth and deconvolve a shape for compound features. The usual form is employed:[24]

$$P_G(t, t_0, \sigma) = A \exp\left[-\frac{1}{2}\left(\frac{t - t_0}{\sigma}\right)^2\right], \qquad (1)$$
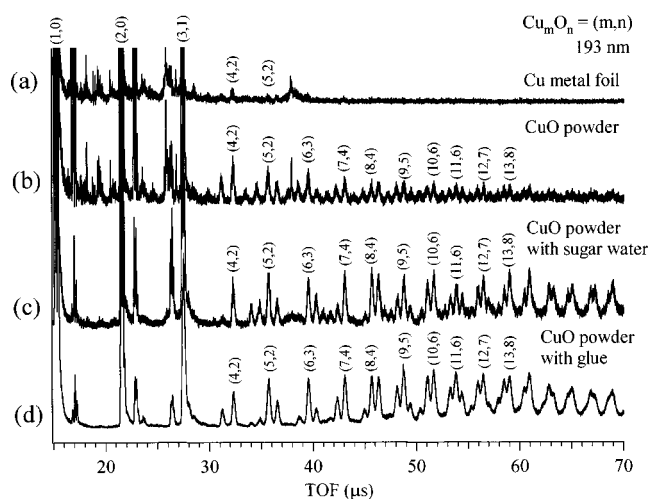

FIG. 1. TOF mass spectra of copper oxide clusters obtained by ablation of the four different samples: (a) Copper metal foil, (b) CuO powder, (c) dried CuO powder with sugar water, and (d) dried CuO powder with glue. A 532 nm laser at 2.2 mJ/pulse is used for ablation of the copper metal sample (a) and CuO powder samples (b), (c), and (d) are ablated at ~ 1.0 mJ/pulse. The spectra are obtained by 193 nm (~ 1.0 mJ/pulse) ionization. A carrier gas of 10% O_2 in 100 psig He is employed for expansion and reaction. The feature at 38 μs in spectra (a), (b), and (c) is due to pump oil.

where σ is the Gaussian width of the feature, and it is related to the full width at half maximum (FWHM) for the feature $\Delta \tau_{1/2} = 2\sqrt{2 \ln 2}\sigma = 2.355\sigma$.

The time scale over which one can observe fragmentation of neutral copper oxide clusters during the ionization process is ~ 1 ns to 2 μs; the fragmentation process is evident most effectively in the time-of-flight mass spectroscopy (TOFMS) linewidth for the mass spectral features. Given the cluster sizes encountered, the excess energy placed in the clusters by ionization laser multiphoton absorption, and the Cu–O bond energy (2.79 eV),[25] most fragmentation reactions can be expected to fall into this time window. One can expect, therefore, that linewidths > 10 ns for small clusters (Cu_mO_n, $m < 10$) and > 20 ns for larger clusters (Cu_mO_m, $m > 10$) are associated with clusters that are generated by some fragmentation process. The minimum linewidth expected for a seeded Nd/YAG should be $\sim 8–10$ ns, which is the pulsewidth of the laser.

III. RESULTS AND DISCUSSION

Figure 1 shows the time-of-flight (TOF) mass spectra of copper oxide clusters obtained by ablating different samples of copper material: [Fig. 1(a)] Copper metal foil, [Fig. 1(b)] CuO copper(II) oxide powder, [Fig. 1(c)] dried CuO powder with sugar water, and [Fig. 1(d)] dried CuO powder with glue. The powder samples, with or without solvent, are pressed onto the drum and smoothed with a razor blade both before and after drying. A smooth surface is important for reproducible cluster intensity.

Only small clusters, Cu_mO ($m \leq 3$) are observed in the mass spectrum obtained by ablating copper metal foil. On the other hand, spectra obtained by ablating CuO powder samples are quite rich in $Cu_mO_n^+$ clusters to $m > 20$. These results imply that ablated metal species Cu_m (m

J. Chem. Phys., Vol. 120, No. 9, 1 March 2004
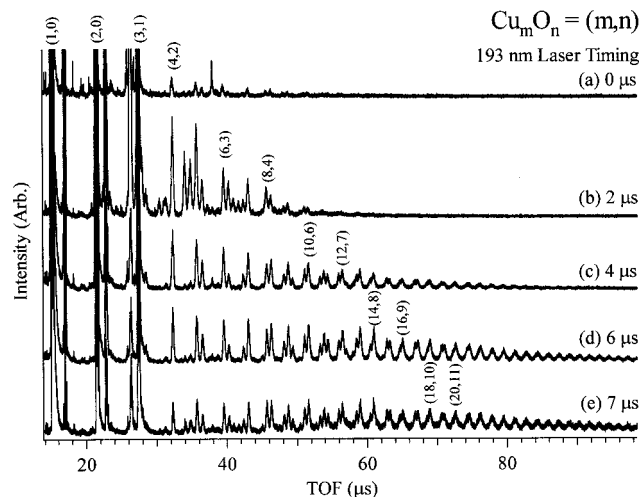
Copper oxide cluster distribution   4167

FIG. 2. TOF mass spectra of copper oxide clusters obtained by different ionization laser timing of the 193 nm laser (1.1 mJ) at (b) 2, (c) 4, (d) 6, and (e) 7 μs delayed from experimental conditions of (a). $t=0$ μs is set for the maximum intensity of Cu and Cu_2, and the only timing of the ionization laser with respect to the nozzle opening and ablation laser firing times is changed. A CuO with sugar water sample is ablated with 1.0 mJ/pulse at 532 nm and expansion gas of 100 psig 10% O_2/He mixture gas is employed.
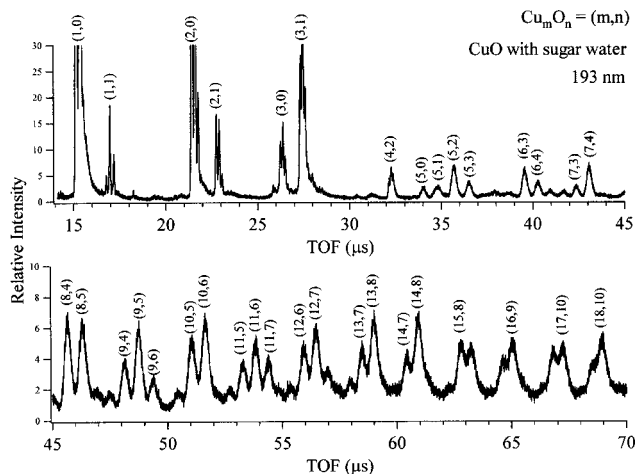

FIG. 3. Expanded TOF mass spectrum of copper oxide clusters in Fig. 1(c) and detailed assignments of observed mass peaks are indicated.

$=1,...,20,...$) are not very reactive with oxygen molecules in the expansion gas. The various samples of copper oxide powder (sugar water, glue, plain) give essentially the same mass spectral distribution of $Cu_mO_n^+$ as detected with 193 nm laser ionization (~ 1.0 mJ/pulse), even though both glue and sugar water contain oxygen. One can, therefore, conclude that most of the oxygen in the copper oxide clusters comes from the CuO powder. The different distribution of cluster features for the three powder samples [Figs. 1(b)–1(d)] are due solely to slightly different experimental parameters (e.g., laser/nozzle timing) employed for the different spectra. Ablation of Cu_2O powder gives mass spectra similar to those of Fig. 1(a) for Cu metal ablation.

Figure 2 shows how ionization laser timing (193 nm) relative to the nozzle opening and ablation laser firing can affect the observed cluster ion distribution. Larger clusters are observed with increased delay of the ionization laser pulse. This indicates that arrival time of clusters of each size is a function to some degree of their mass. This delayed arrival time can be due to a velocity difference in the beam for large and small clusters and/or a slower production kinetics for larger clusters.

Figure 3 shows TOF mass spectra of copper oxide clusters presented for an expanded mass scale for assignment purposes. This spectrum is the same as Fig. 1(c). The structure found at each mass peak is due to isotopes of copper: ^{63}Cu (natural abundance, 69.17%) and ^{65}Cu (natural abundance, 30.83%). For small clusters, the series $(Cu_2O)_x^+$, $x=1, 2, 3$, and $Cu(Cu_2O)_x^+$, $x=1, 2$, are observed. With increasing cluster size, the series $(Cu_2O)_xO^+$, $x=4, 5, 6, ...$, for copper oxide clusters with an even number of copper atoms, and $(CuO)(Cu_2O)_x^+$, $x=3, 4, 5...$, for copper oxide clusters with an odd number of copper atoms, are most intense. Copper oxide clusters of the form $Cu_mO_n^+$ ($m \leqslant n$) are

not observed with 193 nm (multiphoton, fragmenting) ionization.

Figure 4 presents the TOF mass spectra of copper oxide clusters obtained by laser ablation of a sample of dried copper oxide powder with sugar water expanded with 100% He. All of the oxygen in these clusters comes from oxygen in the original copper oxide powder; sugar and water do not add oxygen to the clusters as determined by comparison with spectra from the glue based and plain copper oxide samples. Ablation laser timing with regard to the nozzle opening and ionization laser firing times does have an effect on the observed cluster ion distribution. These spectra demonstrate that the reaction between Cu and O in the plasma plume, generated by the ablation process, is influenced by the He
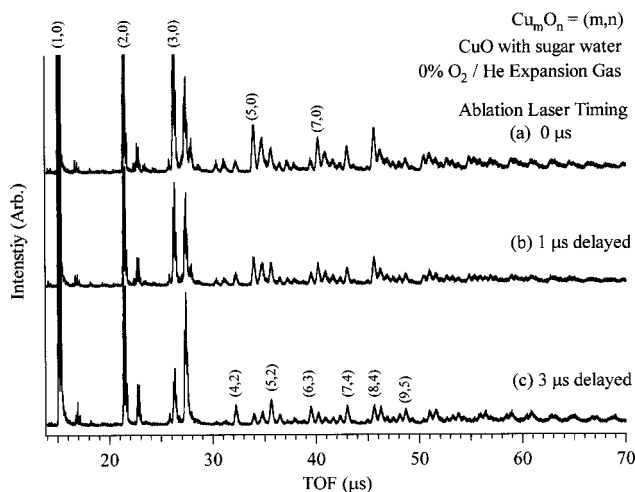

FIG. 4. TOF mass spectra of copper oxide clusters from 100 psig He expansion gas, ablating CuO with sugar water sample by 532 nm laser at 1 mJ/pulse. Spectra are measured with (b) 1 and (c) 3 μs delayed ablation laser timing from the experimental conditions of (a), and with 193 nm ionization (1 mJ/pulse). Condition $t=0$ of spectrum (a) is set to have maximum signal intensity of Cu_m clusters. Valve opening and 193 nm laser timing are fixed. Note that the time delay between the nozzle opening and the laser ablation causes a change in the neutral cluster distribution in the cluster beam, and that O_2 in the expansion does not have a significant effect on the neutral cluster distribution [see Figs. 2 and 4(c)].
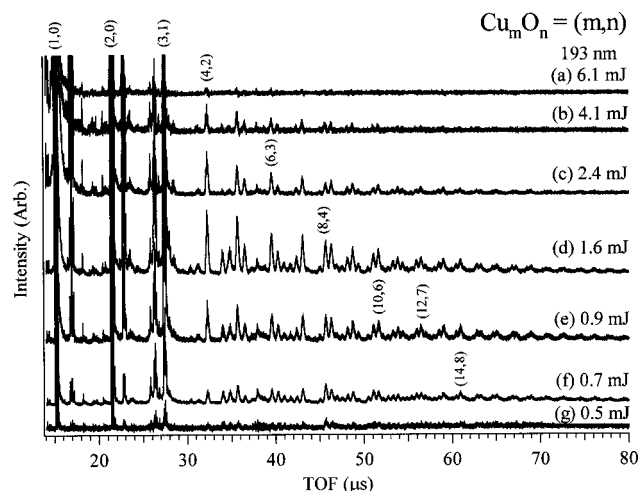
FIG. 5. TOF mass spectra of CuO clusters obtained by different 193 nm ionization laser energy/pulse: (a) 6.1, (b) 4.1, (c) 2.4, (d) 1.6, (e) 0.9, (f) 0.7, and (g) 0.5 mJ/pulse. A CuO powder with sugar water sample and 10% O_2/90% He expansion gas are employed.
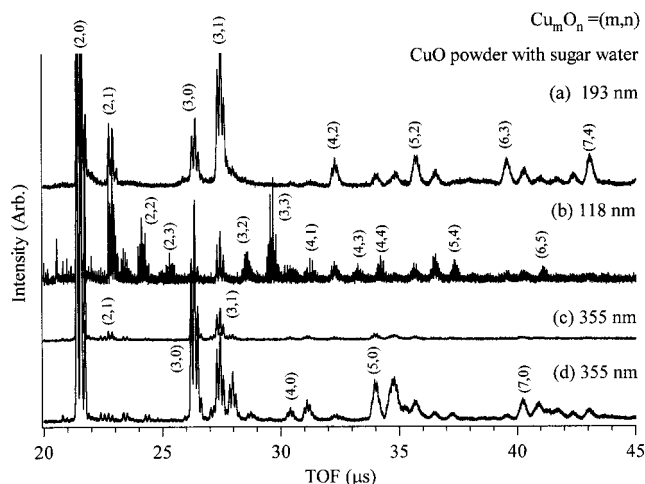

FIG. 6. TOF mass spectra of CuO with 100 psig 10% O_2/90% He measured by (a) 193 (1 mJ/pulse), (b) 118 (generated by 355 nm of 24 mJ/pulse), (c) 355 nm (24 mJ/pulse) ionization [with optimized conditions for (b)], and (d) 355 nm (24 mJ/pulse) (under optimized conditions for 355 nm ionization with nozzle and ablation parameters unchanged). A CuO powder with sugar water sample is employed. The mass spectrum for 118 nm ionization also contains features generated by 355 nm ionization.

pressure and flow (perhaps cooling) over the ablation site. The cluster distribution in the spectrum of Fig. 4(c) is the same as that taken with 10% O_2/90% He expansion gas shown in Figs. 1(c) and 3. Thus, the oxygen content of expansion gas has little effect on the observed cluster ion distribution as detected by 193 nm ionization. In fact, ablation of Cu metal and Cu_2O powder does not generate sufficient oxygen in the plasma to enable the growth of Cu_mO_n clusters beyond $m=5$, $n=2$ [see Fig. 1(a) as an example].

Figure 5 presents TOF mass spectra as a function of 193 nm laser energy/pulse. Spectra in Figs. 5(a)–5(g) are obtained for all the same experimental conditions except ionization laser energy. At laser energy/pulse greater than 1.6 mJ/pulse, Fig. 5 shows that the observed cluster intensity decreases until, at ~6 mJ/pulse, clusters larger than Cu_3O are not present in the TOF mass spectra with significant intensity above background. At ionization laser energy/pulse below 1.6 mJ/pulse, the observed spectra of cluster ions simply uniformly decrease with reduced energy/pulse. Recall, too, that the cluster ion distribution can be tuned between large and small clusters by adjusting ionization laser timing. Therefore, one can conclude that large cluster fragmentation to small clusters by losing several Cu and O atoms (or CuO units) is not a major process in this system for ionization laser energies/pulse between 1.6 and 0.5 mJ/pulse. Such a result is consistent with our findings for the iron oxide cluster system and also with Rice–Ramsperger–Kassel–Marcus theory calculations for zirconium oxide clsuters.[1,2,26]

Figure 6 presents the TOF mass spectra of copper oxide clusters obtained with different ionization laser wavelengths. Figure 6(a) is obtained at 193 nm, Fig. 6(b) is obtained at 118 nm, and Figs. 6(c) and 6(d) are obtained at 355 nm ionization laser wavelengths. The sample is dried CuO powder with sugar water. The spectrum of Fig. 6(b) is not purely due to 118 nm ionization because the ionization beam contains both the third harmonic of Nd/YAG fundamental (355 nm) and the third harmonic of the 355 nm light (118 nm). The 118 nm beam is focused to ~50 μm and the 355 nm

beam is defocused to ~8 mm.[11] Features in the 118 nm single photon ionization spectrum that are due to 355 nm multiphoton ionization can be identified by evacuating the Xe/Ar gas cell and using only 355 nm radiation for ionization and by observing the mass spectra linewidths of the various features (discussed below). In particular, most of the intensity for Cu_2^+, Cu_3O^+, $Cu_4O_2^+$, and $Cu_5O_2^+$ is due to 355 nm ionization, as can be seen from a comparison of Figs. 6(b)–6(d). For the 118 nm spectrum [Fig. 6(b)], the abundant clusters are Cu_2O_2, Cu_2O_3, Cu_3O_2, Cu_3O_3, Cu_4O_3, Cu_4O_4, Cu_5O_4, Cu_6O_5, etc. These latter features are not observed with 193 or 355 nm ionization. Note, too, that the 118 nm ionization signals are composed of sharp features (to be assigned below). With 118 nm ionization, the uniquely observed and abundant clusters are mostly of the form Cu_mO_m and Cu_mO_{m-1}. 193 and 355 nm multiphoton ionization spectra are due mostly to fragmentation of neutral clusters by loss of oxygen atoms to generate the Cu_m^+ and $Cu_{2m}O_m^+$ cluster series. Persson et al.[9] reported the ionization energies of Cu_m and Cu_mO_2 ($m=15–46$) clusters determined by two-color two-photon ionization. According to their results, the ionization energy of Cu_m and Cu_mO_2 ($m=15–46$) is ~5.4 eV. Cu_mO_2 ($m=15–46$) can be estimated to have similar electronic properties to Cu_m. Cu_mO_m ionization energies have not been reported; however, ionization energy of copper oxide clusters Cu_mO_m can be expected to be between 7 and 10 eV based on a knowledge of ionization for other metal oxide clusters. Thus, one photon of the 6.4 eV and 3.5 eV lasers will not be enough energy for ionization of most species Cu_mO_m with $m<25$; multiphoton absorption for most metal oxide clusters is quite intense. A further demonstration of such fragmentation during the neutral cluster ionization process is given in Figs. 7 and 8, which show detailed 118 nm ionization (plus some 355 nm ionization) assignments and linewidths at high dispersion. The sample is copper oxide with sugar water and the spectrum is
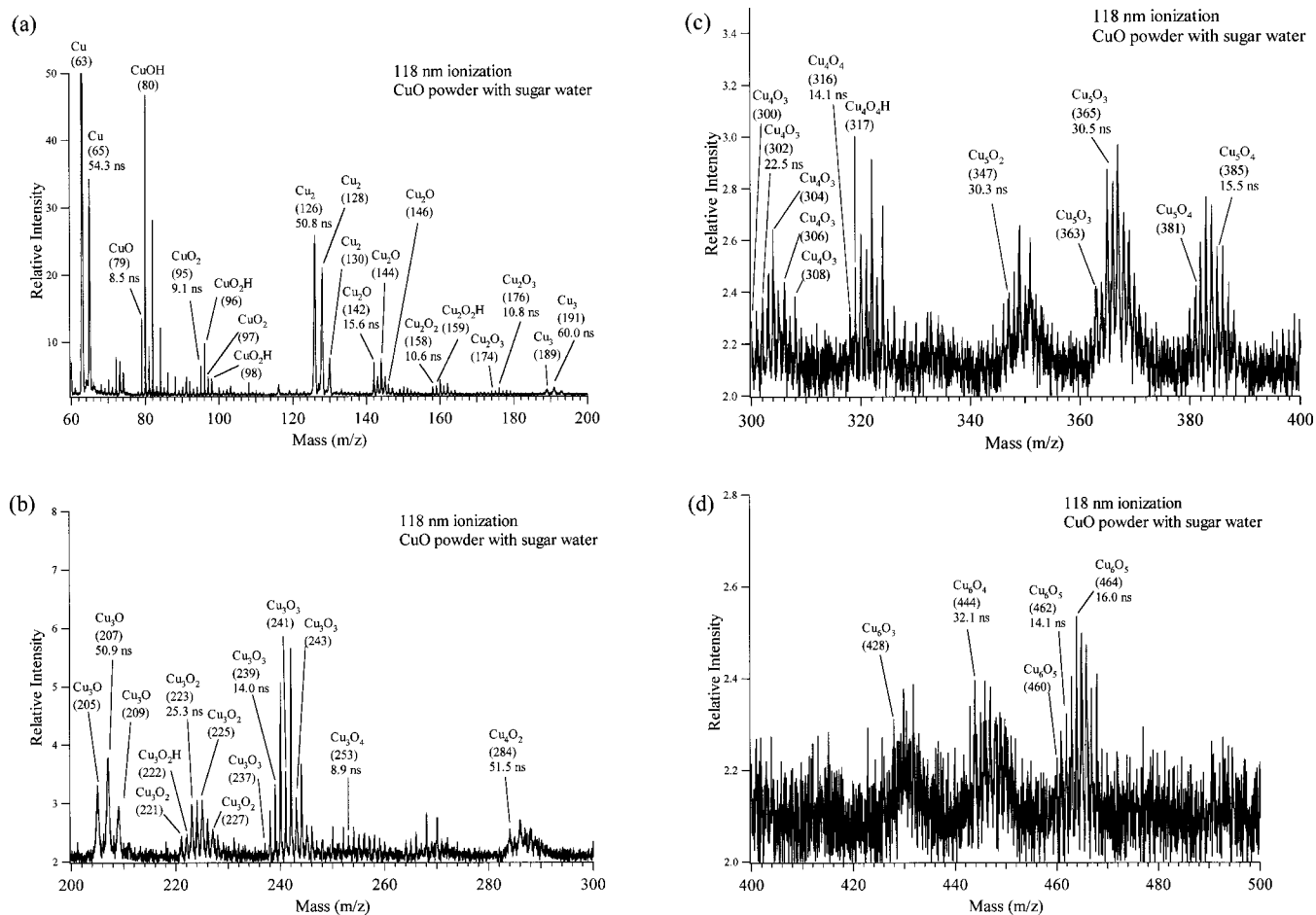
FIG. 7. 118 nm ionization TOF mass spectra [see Fig. 6(b)] with expanded dispersion and assignments of mass peaks. Cu_2^+, Cu_3O^+, $Cu_4O_2^+$,..., are generated by 355 nm and they are due to fragmentation. Numbers in parentheses are mass numbers of observed peaks. ns indications give FWHM of mass peaks obtained by fitting a Gaussian function to the features.

that presented in Fig. 6(b), but with much greater dispersion. One can observe clusters containing hydrogen atoms (Cu_mO_nH) as well as copper oxide clusters. These latter additional features may also be present for 193 nm ionization spectra, but the fragmentation linewidths mask their presence. Very few, if any, of the clusters contain a carbon atom. Even at this dispersion, one can see the difference between 118 and 355 nm ionization [e.g., compare Cu_3O^+ and $Cu_3O_3^+$ features in Fig. 7(b)]. Of course, larger clusters will tend to have larger linewidths simply due to the resolution nonlinearity of the TOFMS, but in this mass region, the effect of cluster fragmentation on the mass peak linewidths is quite obvious. Peak widths are indicated in the figures in ns.

Figure 8 shows further expanded spectra of the [Fig. 8(a)] CuO_2, [Fig. 8(b)] Cu_2O_2, and [Fig. 8(c)] Cu_5O_4 regions of Figs. 6(b) and 7. The peak widths [full width at half maximum (FWHM) $= \Delta \tau_{1/2}$] are written in Fig. 8 in ns: These widths are obtained by the Gaussian fitting as given in Eq. (1). Some of the features are seen to have a compound linewidth (e.g., $^{65}Cu_2O_2^+$), which implies a contribution to the 118 nm ionization feature from 355 nm ionization fragmentation. Extra width for some of the features may also come from the overlap between clusters of different isotope and hydrogen contents. The sharp 118 nm ionization features for small clusters are limited in linewidth by the laser focal

size and pulsewidth. The FWHM for CuO_2 features [Fig. 8(a)] are ~ 10 ns, the laser width in time. For sharp, laser pulsewidth limited TOFMS features, the spectra are a measure of the abundance of the observed clusters in the neutral cluster distribution.

Figure 9 shows the mass peaks of Cu_2O_n ($n=0-3$) clusters and their FWHM, which are obtained by fitting a Gaussian distribution function to each peak. The Cu_2^+ feature has an ~ 50 ns FWHM, while the FWHM for Cu_2O_2 and Cu_2O_3 features are ~ 10 ns. As mentioned above, the former feature is due to multiphoton fragmentation, and the latter features can be assigned to species ionized by a single photon. The linewidth of Cu_2O^+ ($\Delta t_{1/2}=15.6$ ns) might contain components of both multiphoton fragmentation and single photon ionization. Thus, the observed oxygen poor cluster features can have contributions from multiphoton fragmentation due to 355 nm ionization, as well as from 118 nm nonfragmenting single photon ionization. On the other hand, oxygen rich clusters are ionized by a single photon of 118 nm with no fragmentation. Note that the same tendencies are seen for the series CuO_n, Cu_3O_n, Cu_4O_n,..., as shown in Fig. 7. These results show that fragmentation by 355 nm ionization occurs locally within a series Cu_mO_n with m fixed: $Cu_mO_n \rightarrow Cu_mO_{n-1}$ or Cu_mO_{n-2}. Apparently, fragmentation
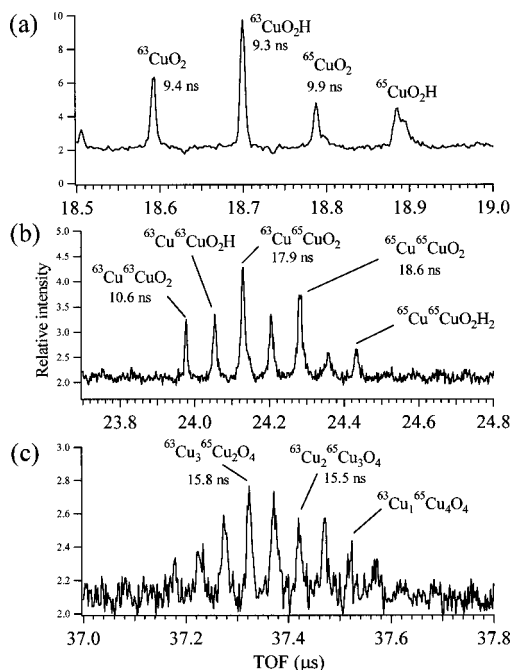
FIG. 8. Expanded TOF mass spectra (118 nm ionization) in the (a) CuO_2, (b) Cu_2O_2, and (c) Cu_5O_4 mass region. ns indications give FWHM of mass peaks obtained by fitting a Gaussian function to the feature. Superscripts 63 and 65 indicate mass of isotopes of copper. Spectrum (a) shows the features are laser linewidth (in ns) limited and that the CuO_2H feature may contain a fragmentation component from CuO_2H_2. Spectrum (b) shows a $^{63}Cu_2O_2$ laser linewidth limited feature. Other features in this spectrum may have components from $Cu_2O_2H_{1,2}$ degenerate with $^{63}Cu^{65}CuO_2$ and $^{65}Cu_2O_2$ and may have linewidth contributions from $Cu_2O_2H_{2,3} \rightarrow Cu_2O_2H_{2,1}^+$ fragmentation. Spectrum (c) shows homogeneous linewidth broadening of the features due to TOFMS resolution for amu ~700.
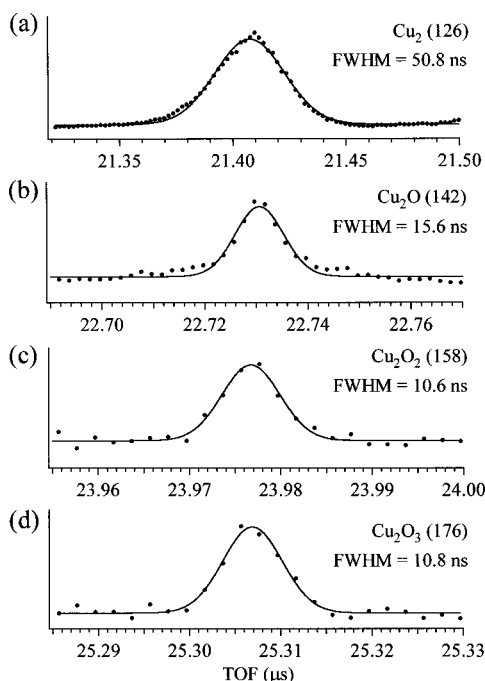

FIG. 9. TOF mass peaks (dots) of (a) $^{63}Cu_2$, (b) $^{63}Cu_2O$, (c) $^{63}Cu_2O_2$, and (d) $^{63}Cu^{65}CuO_3$ and Gaussian distribution function fits (solid lines). These features are the same as those in Fig. 7. The mass peaks are obtained by a 500 M samples/s data acquisition rate.

with loss of a Cu atom does not occur (under these ionization conditions). The same fragmentation scheme is also indicated in the comparison of mass spectra measured by different wavelengths in Fig. 6. While $\sim Cu_mO_m$ clusters are observed with 118 nm ionization [Fig. 6(b)], these clusters are not observed with 193 nm [Fig. 6(a)] and 355 nm ionization [Figs. 6(c) and (d)]. Thus, the most abundant neutral clusters of the form Cu_mO_n ($n=m, m+1$, $m<4$; $n=m-1$, $m \geqslant 5$) are not readily observed by 193 and 355 nm multiphoton ionization due to cluster fragmentation. Such species are only observed by single photon, nonfragmenting 118 nm laser ionization. The $Cu_mO_{m/2}^+$ and Cu_m^+ clusters are only generated in the multiphoton ionization process and thus, are not part of the neutral cluster distribution.

Therefore, Cu_mO_m, $m=2, 3, 4$, clusters are thermodynamically stable in the neutral cluster distribution. With 118 nm laser ionization, mass peaks of Cu_mO_n clusters ($m \sim n$) are observed with narrow widths: CuO_2, Cu_2O_x ($x=2, 3$), Cu_3O_x ($x=3, 4$), Cu_4O_x ($x=3, 4$), Cu_5O_4, and Cu_6O_5. Larger clusters surely are present but are not at very high concentration, and the 118 nm intensity is only $\sim10^{11}$ photons/pulse; thus, Cu_mO_n clusters for $m>6$ have very little intensity for 118 nm detection. These features are due to single photon ionization and represent the most abundant neutral clusters in the supersonic expansion/laser ablation beam. Note that features for $Cu_6O_4^+$ [Fig. 7(d)] are probably too broad to be associated with the neutral cluster distribution alone and probably contain some intensity from a fragmentation event.

Ablation of copper metal and Cu_2O powder does not give rise to large Cu_mO_n clusters as detected with 355, 193, or 118 nm ionization: Only clusters with $m<4$ could be observed for these samples and 10% O_2/90% He expansion gas. Ablated Cu_m must not be very reactive with O_2 molecules. The growth process for Cu_mO_n clusters must be of the form $CuO+CuO+...$ or of the form $Cu+O$ in the plasma created by ablating both copper and oxygen species. Perhaps the reaction is efficient only at high (plasma) temperatures.

IV. CONCLUSIONS

Laser ablation of copper and copper oxide samples has been employed to generate copper oxide clusters in a supersonic expansion. Ionization with 118 nm radiation demonstrates that neutral cluster fragmentation does not occur by this single photon process. We are thereby able to draw the following conclusions concerning the neutral cluster distribution created in the supersonic expansion.

(1) Ablation of copper metal in the presence of molecular oxygen gives mostly Cu_m clusters, with only Cu_mO_n observed for $m<4$ and $n \sim 1, 2$.

(2) For ablation of CuO powder samples, the observed clusters in the distribution depend on the ionization laser wavelength. With 193 nm multiphoton, neutral cluster fragmenting ionization, the observed cluster ion distribution is roughly of the form $Cu_{2m}O_m^+$ for $4 \leqslant m \leqslant 20$ and at 355 nm multiphoton, neutral cluster fragmenting ionization, the observed cluster ion distribution is roughly of

    the form Cu_m and $Cu_mO_{1,2}$, for $m \lesssim 10$. For both of these laser wavelengths, extensive neutral cluster fragmentation occurs due to multiphoton absorption processes.

(3) With 118 nm single photon ionization for a copper oxide powder sample, the most abundant neutral clusters are of the form Cu_mO_m for $m \leq 4$ and Cu_mO_{m-1} for $m > 4$. Based on mass spectral feature linewidths, the series of clusters uniquely observed with 118 nm ionization represent the true neutral cluster distribution for Cu_mO_n in the beam. These cluster series are then the thermodynamically stable ones for the neutral cluster distribution.

(4) The observed cluster fragmentation by 193 nm is therefore mainly of the form Cu_mO_m and Cu_mO_{m-1} $\rightarrow Cu_mO_n$ with $n = m/2$, $m/2 + 1$.

(5) The cluster growth mechanism for the copper oxide cluster system is suggested to be $mCu + nO$ (ablated) $\rightarrow Cu_mO_n$ and/or $mCuO \rightarrow Cu_mO_{m,m-1,...}$. In both instances, the reactions must occur with the copper and oxygen atoms generated in the plasma created by laser ablation. Oxygen atoms in the clusters come from the ablated sample and not the carrier gas.

ACKNOWLEDGMENTS

[1] M. Foltin, G. J. Stueber, and E. R. Bernstein, J. Chem. Phys. **111**, 9577 (1999).

[2] M. Foltin, G. J. Stueber, and E. R. Bernstein, J. Chem. Phys. **114**, 8971 (2001).

[3] J. R. Gord, R. J. Bemish, and B. S. Freiser, Int. J. Mass Spectrom. Ion Processes **67**, 229 (1985).

[4] C. Ma, H. Li, X. Zhang, J. Bai, X. Wang, L. Wang, G. Zhang, G. He, and N. Lou, Prog. Nat. Sci. **6**, 159 (1996).

[5] L.-S. Wang, H. Wu, S. R. Desai, and L. Lou, Phys. Rev. B **53**, 8028 (1996).

[6] H. Wu, S. R. Desai, and L.-S. Wang, J. Phys. Chem. A **101**, 2103 (1997).

[7] G. C. Nieman, E. K. Parks, S. C. Richtsmeier, K. Liu, L. G. Pobo, and S. J. Riley, High. Temp. Sci. **22**, 115 (1986).

[8] G. von Helden, A. Kirilyuk, D. van Heijunsbergen, B. Sartakov, M. A. Duncan, and G. Meijer, Chem. Phys. **262**, 31 (2000).

[9] J. L. Persson, M. Andersson, L. Holmgren, T. Åklint, and A. Rosen, Chem. Phys. Lett. **271**, 61 (1997).

[10] D. N. Shin, Y. Matsuda, and E. R. Bernstein, J. Chem. Phys. **120**, 4150 (2004) (this issue).

[11] D. N. Shin, Y. Matsuda, and E. R. Bernstein, J. Chem. Phys. **120**, 4157 (2004) (this issue).

[12] N. López, F. Illas, and G. Pacchioini, J. Phys. Chem. B **103**, 8552 (1999).

[13] S. F. Vyboischikov and J. Sauer, J. Phys. Chem. A **105**, 8588 (2001).

[14] M. Anstrom, N.-Y. Topsøe, and J. A. Dumesic, J. Catal. **213**, 115 (2003).

[15] Q. Wang, Q. Sun, M. Sakurai, J. Z. Yu, B. L. Gu, K. Sumiyama, and Y. Kawazoe, Phys. Rev. B **59**, 12672 (1999).

[16] A. W. Castleman, Jr. and K. H. Bowen, Jr., J. Phys. Chem. **100**, 12911 (1996).

[17] K. A. Zemski, D. R. Justes, and A. W. Castleman, Jr., J. Phys. Chem. B **106**, 6136 (2002).

[18] S. A. Mitchell, L. Lian, D. M. Rayner, and P. A. Hackett, J. Chem. Phys. **103**, 5539 (1995).

[19] L. Holmgren, M. Andersson, and A. Rosen, Chem. Phys. Lett. **296**, 167 (1998).

[20] (a) I. A. Fisher and A. T. Bell, J. Catal. **178**, 153 (1998); (b) R. A. Köppel, C. Stöcker, and A. Baiker, J. Catal. **179**, 515 (1998).

[21] J. B. Reitz and E. I. Solomon, J. Am. Chem. Soc. **120**, 11467 (1998).

[22] (a) Y.-J. Huang and H. P. Wang, J. Phys. Chem. A **103**, 6514 (1999); (b) Y. Chi and S. S. C. Chuang, J. Catal. **190**, 75 (2000).

[23] (a) G. V. Chertihin, L. Andrews, and C. W. Bauschilicher, Jr., J. Phys. Chem. A **101**, 4026 (1997); (b) M. Zhou and L. Andrews, *ibid.* **104**, 2618 (2000).

[24] P. R. Bevington and D. K. Robinson, *Data Reduction and Error Analysis for the Physical Sciences*, 2nd ed. (McGraw–Hill, New York, 1992).

[25] J. B. Pedley and E. M. Marshall, J. Phys. Chem. Ref. Data **12**, 967 (1984).

[26] D. F. Kelley and E. R. Bernstein, J. Phys. Chem. **90**, 5164 (1986).